

High energy xenon ion beam assisted deposition of TiN film and its industrial application

XI WANG, GENQING YANG, XIANGHUI LIU, ZHIHONG ZHENG, WEI HUANG, SHICHANG ZOU

Ion Beam Laboratory, Shanghai Institute of Metallurgy, Chinese Academy of Sciences, Shanghai 200 050, People's Republic of China

P. J. MARTIN, A. BENDAVID

CSIRO Division of Applied Physics, Sydney, NSW 2070, Australia

J. G. HAN, J. S. YOON

Plasma Applied Materials Laboratory, Sung Kyun Kwan University, Korea

TiN films have been synthesized by ion beam assisted deposition employing xenon ions with an energy of 40 keV. The formed TiN films were investigated systematically in respect of surface morphology, composition, structure and mechanical properties. Then, they were applied to surface protection of scoring dies. Atomic force microscopy and interferometric observation showed that the TiN film is relatively smooth. Rutherford backscattering spectroscopy analysis indicated that few xenon atoms are retained in the film. It was found by transmission electron microscopy and X-ray diffraction experiments that the formed TiN is a nanocrystal (< 10 nm) film and exhibits slightly (200) preferred orientation. An ultra low load microhardness indenter system was used to examine the plastic property of the film and a hardness of 2300 kgf mm^{-2} was calculated from the measured data. Scratch tests showed that the adhesion of TiN film deposited by ion beam assisted deposition at ambient temperature is superior to that of high temperature physical vapour deposited (PVD) TiN film. Both a pin-on-disk tribotest and SRV wear test revealed that the wear resistance of the specimen can be greatly improved by TiN coating. A five times increase of service life of different scoring dies could be obtained by protection of TiN coating.

1. Introduction

The properties of thin film may be controlled and improved by bombarding the growing film with energetic particles [1, 2]. One of the common techniques achieving bombardment is ion beam assisted (enhanced) deposition (IBAD), in which material is evaporated by electron beam bombardment or ion beam sputtering and the depositing film is irradiated with an ion beam. According to the energy regime of the employed ion beam, IBAD can be divided into low energy (several tens eV to 1 keV) IBAD and high energy (1 keV to several tens keV) IBAD. Low energy IBAD is usually used in fabrication of optical and microelectronic films owing to light damage or few defects in the films [3]. Whereas, high energy IBAD is often developed for the purpose of preparing mechanical films, which need strong adhesion to the substrate [4–6]. When the IBAD process is carried out on a background of reactive gas, this procedure is referred to as reactive ion beam assisted deposition (RIBAD). In this method, the ion beam could be a reactive ion beam, such as O^+ , N^+ and C^+ or as inert gas ion beam, such as Ar^+ , Kr^+ and Xe^+ .

The present authors have prepared TiN films by IBAD using a high energy N^+ ion beam (N^+ -IBAD),

the formed TiN film exhibited good wear resistance and strong adhesion to the substrate, but the hardness of the film was lower than that prepared by PVD or chemical vapour deposition (CVD) [7]. This is consistent with other authors' results [5, 6]. The phenomenon was explained from the viewpoint of the energy distribution deposited by incident ions. N^+ ions with 40 keV energy penetrate to a depth of more than 150 nm in the TiN film. This means that the N^+ ions deposit energy over a large area, so the density of the deposited energy in the elastic collision cascades is very low, the energy lost at the near surface area is also low. All these are not favourable to the nucleation and growth of the film, which in turn results in the imperfection of lattice structure in the formed film. Based on the above analysis, improved hardness of TiN films was expected by employing heavy Xe^+ ions, which deposit much energy at the surface area and give much higher density of the deposited energy.

In this work, TiN films have been synthesized by high energy Xe^+ -RIBAD. The formed TiN films were then investigated with respect to topography, surface roughness, composition, crystal structure, microhardness, adhesion and wear behaviour. Finally, the TiN films were applied to the surface protection of scoring dies.

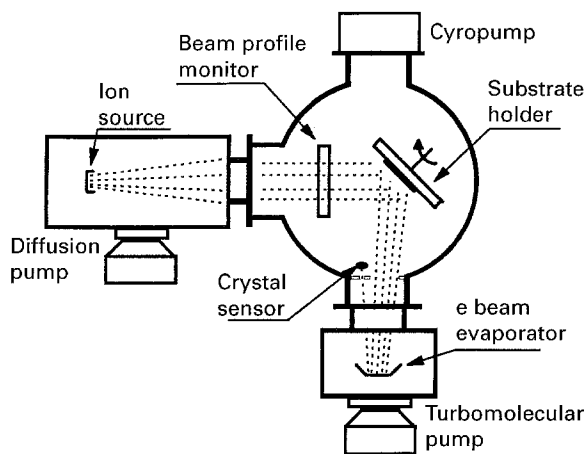


Figure 1 Schematic of the IBAD system.

2. Experimental procedure

2.1. Film preparation

Fig. 1 is the schematic representation of the IBAD system. Ti vapour obtained from an electron beam evaporator was deposited onto a substrate mounted on a water cooled substrate holder. The normal to the holder made an angle of 45° with the evaporative flux. The Ti deposition rate was measured with a quartz crystal monitor. The signal from this monitor was supplied to a computer, which could feedback control of the evaporation rate so that the deposition rate was held constant during the process. The deposition rate in this work was chosen as 1 nm s^{-1} .

The Xe^+ ion beam extracted from an arc discharge-type ion source entered the deposition chamber horizontally and also made an angle of 45° with the substrate normal. The energy of the ion beam was kept at 40 keV. In order to obtain uniform ion bombardment over a large area, the ion implanter was operated in the scan mode. The ion beam current density calculated from the scan area and the ion current, which was measured by a Faraday cup, was $40 \mu\text{A cm}^{-2}$. Under this condition, the ion: atom arrival rate ratio was approximately 0.1.

After the deposition chamber was evacuated by a cyropump to a base pressure of $6.5 \times 10^{-5} \text{ Pa}$, pure N_2 gas was introduced into the chamber via a leak valve (180 mm under the substrate holder). In this study no attempt was made to change the N_2 partial pressure in the chamber, and the optimized N_2 partial pressure [8] of $8 \times 10^{-4} \text{ Pa}$ was chosen.

Glassy graphite, Si wafers, 9Cr18 and SKD-11 steel blocks were chosen as substrates. The substrates were polished to mirror-like status and then washed in an ultrasonic bath of acetone. Prior to deposition, the substrates were bombarded with 20 keV ions for about 5 min in vacuum in order to sputter the surface oxygen and carbon contamination. The water cooled substrate holder maintained the processing temperature below 200°C .

2.2. Film characterization

The properties of the synthesized films were characterized by a variety of surface sensitive analytical tech-

niques and mechanical tests. The surface morphology of the films was revealed using a Topometrix TMX 2010 scanning probe microscope in contact mode. The surface roughness of the films was assessed using a Wyko Topo 3D non-contact surface profilometer. The composition of the films deposited on graphite substrates was analysed by Rutherford backscattering spectroscopy (RBS). Transmission electron microscopy (TEM) and X-ray diffraction (XRD) experiments were carried out to examine the crystal structure of the films.

The hardness of the films was measured using an UMIS-2000 ultra low load microhardness indenter system, which was developed in CSIRO Division of Applied Physics, Australia. The hardness test was performed with a Berkovich indenter. In a conventional hardness test, the contact area between tip and specimen surface is determined after the load is removed. After removing the load, a partial elastic recovery occurs, so an overestimate of the hardness results. Another disadvantage of the conventional test is that conventional microhardness testers require direct image of the indentations to obtain hardness; large errors are introduced due to the measurement of the diagonal lengths, especially when the indentations are small. The UMIS-2000 system measures the depth of penetration of an indenter as a function of the applied force. So one can obtain the plastic deformation under loading. Moreover, this system has the possibility of determining depth of penetration with resolution less than 1 nm and load resolution less than 0.01 mN. Therefore, the measured hardness data can be greatly improved.

The scratch test was performed to evaluate the adhesion of the film to the substrate. During the scratch test, the friction coefficient between film surface and diamond tip was monitored throughout the procedure and a sharp change in the friction coefficient implied the detachment of the film from the substrate. The load at the moment of the film detachment is called the critical load, which gives a comparable value of film adhesion.

The wear was evaluated in two different tribotesters. The first tribotester was a pin-on-disc machine, in which a stationary Al_2O_3 ball, loaded to 8 N, wore a circular track on a flat which was rotated at a speed of approximately 0.2 ms^{-1} . The second one was an SRV wear tester. During performing, a GCr15 steel ball, 10 mm in diameter, slid against the specimen surface reciprocally. The load applied to the ball was 5 N, the reciprocal frequency was 10 Hz, and the amplitude was 2 mm. A talysurf-5p surface rough sketching apparatus and a scanning electron microscope (SEM) were used to observe and analyse the wear traces. A high precision balance was used to measure the weight loss of the specimens after the tribotest.

3. Results and discussion

3.1. Topography

Fig. 2 is an atomic force microscopy (AFM) image of a formed film. The scans were performed with a $1000 \times 1000 \text{ nm}^2$ scanner. The image implies that

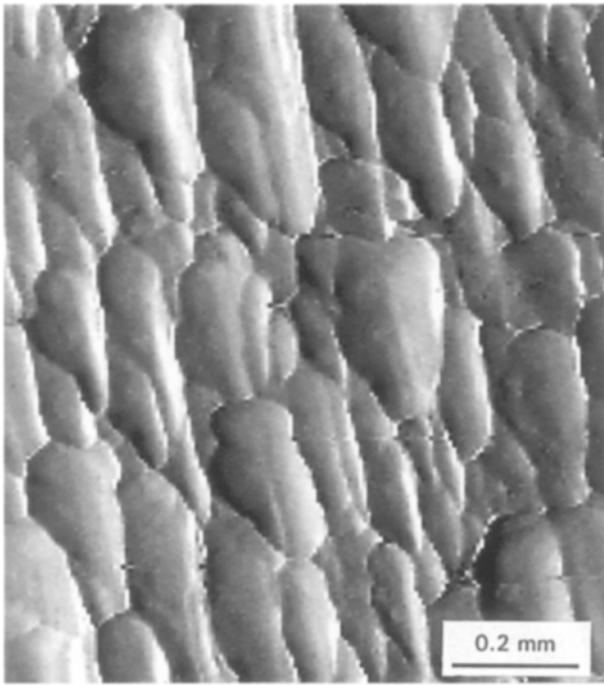


Figure 2 Topography of a TiN film on Si substrate.

the film is composed of large and dense columns separated by deep grooved boundaries, which were

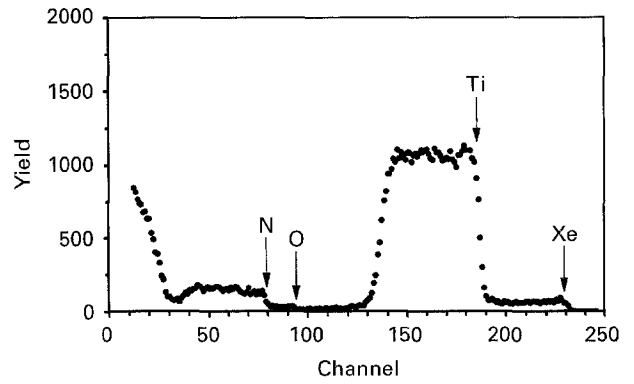


Figure 3 RBS spectrum of a TiN film on graphite substrate.

considered to arise from ion impact-induced surface diffusion enhancement and heavy physical sputtering [9]. The columns clip to the surface due to oblique incidence of ions. Surface roughness analysis by AFM indicated that the surface root-mean-square (RMS) roughness is 0.54 nm. For a larger surface area of $240 \times 240 \mu\text{m}^2$, instead of $1 \times 1 \mu\text{m}^2$ in AFM study, an RMS roughness of 1.51 nm was obtained using the Wyko interferometer. The RMS roughness of the semiconductor grade Si substrate is 0.49 nm.

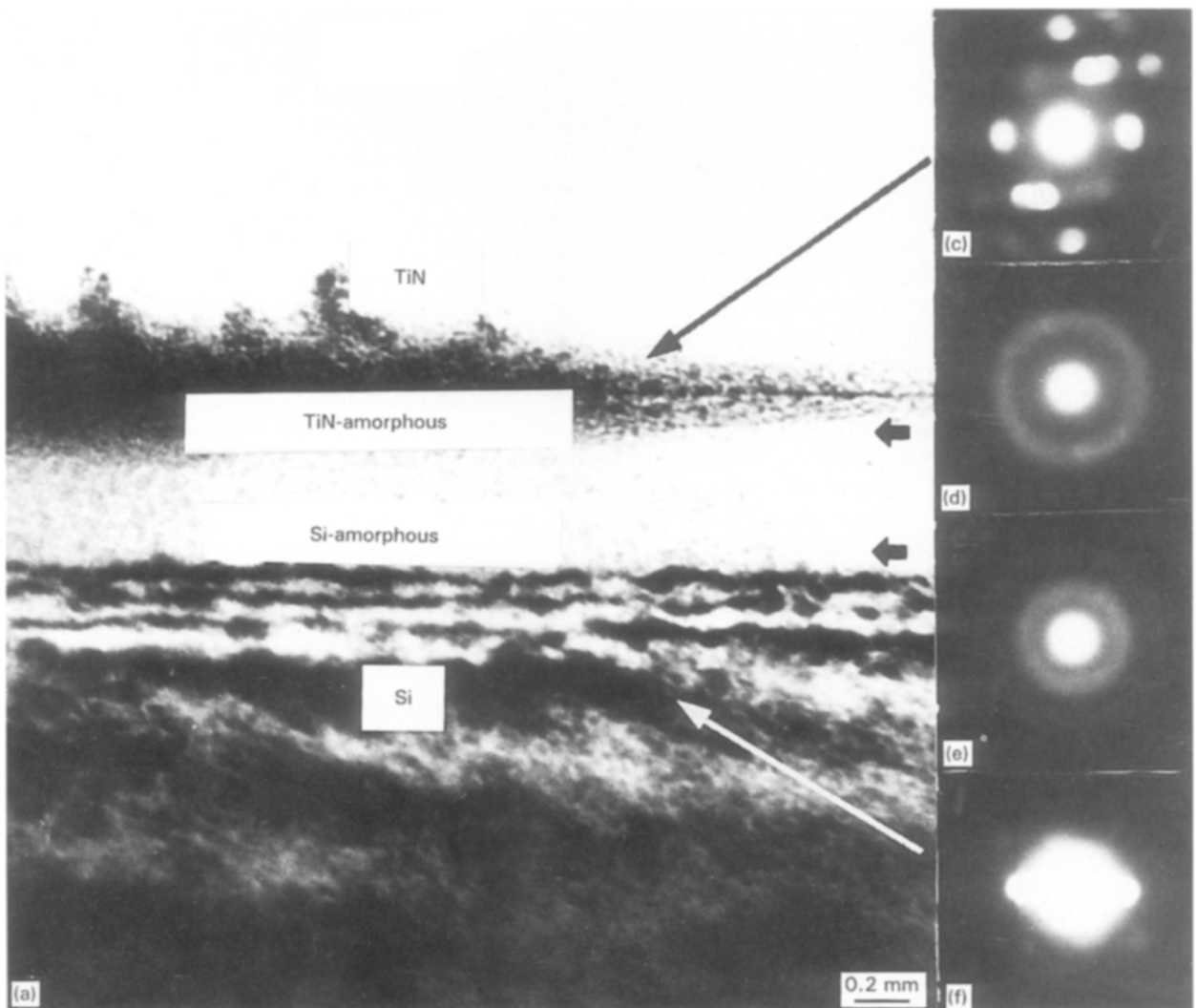


Figure 4 Cross-section micrograph and microdiffraction patterns of a TiN film and Si substrate.

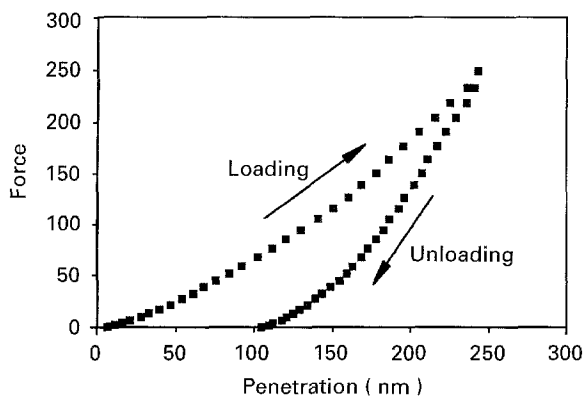


Figure 5 Force penetration curve of a TiN film measured by UMIS.

3.2. Composition

Fig. 3 is an RBS spectrum of a film deposited on a graphite substrate. It can be seen that each component in the film is well distributed. The component ratio of N:Ti in the film determined by the height of each peak is about 0.91. The mechanism of N incorporation into the film under Xe^+ ion bombardment has been reported by the present authors previously [10]. With RBS analysis, Xe atoms retained in the film could also be detected precisely, but the ratio of Xe:Ti is only 0.01, much lower than the atomic arrival rate ratio of the bombarding Xe^+ ions to the deposited Ti atoms (0.1). This fact was considered to arise from the situation that the Xe atoms were ejected from the nearby surface of the film.

3.3. Crystal structure

Fig. 4 is a cross-section micrograph of a film deposited on the Si substrate. Four microdiffraction patterns were obtained across interfacial layers from the film to Si substrate. The microdiffraction pattern corresponding to the film suggests that TiN phase with NaCl-type structure was formed. From XRD analysis, it was also found that the TiN film exhibits slightly (200) preferred orientation. The formed TiN film is a nanocrystal film, the size of the grain is less than 10 nm and quite homogeneous. There is an approximately 80 nm thick amorphous Si and TiN transition layer between the film and substrate.

3.4. Mechanical properties

3.4.1. Microhardness

Fig. 5 shows the force penetration curve for a TiN film obtained in the UMIS test. The film was deposited on a 9Cr18 steel substrate, and its thickness is 2000 nm. The maximum force used was 25 mN. From the force penetration curve, a plastic penetration of 202 nm was obtained [11]. This penetration depth is approximately one-tenth of the film thickness, hence the influence of substrate on the film hardness could be negligible. A hardness of 2300 kgfmm^{-2} was calculated from the maximum force and the plastic penetration. The hardness of the substrate is 700 kgfmm^{-2} , as shown in Fig. 6. Also shown in Fig. 6 is the microhardness of 40 keV N^+ -IBAD TiN film

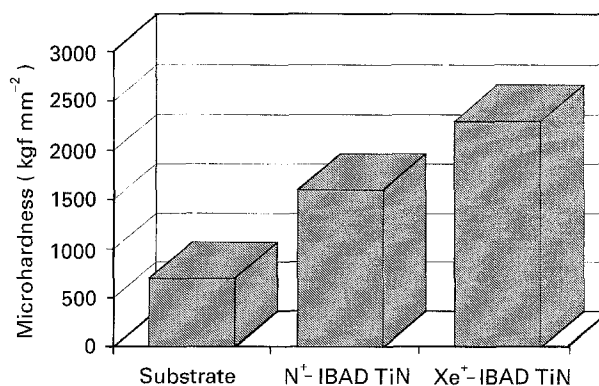


Figure 6 Microhardness of substrate (9Cr18), N^+ -IBAD TiN film and Xe^+ -RIBAD TiN film.

[7]. As expected, Xe^+ -RIBAD TiN films are harder than N^+ -IBAD TiN film. However, it has been previously reported that the hardness of Xe^+ -RIBAD TiN films is very sensitive to the N_2 partial pressure in the deposition chamber [8].

3.4.2. Adhesion

The scratch tests showed that the critical load of 2000 nm thick RIBAD TiN films to the 9Cr18 steel substrates is 42 N, while that of commercial PVD TiN films of the same thickness is only 20 N. This demonstrates that the adhesion of TiN films deposited by RIBAD at ambient temperature is superior to that of high temperature PVD TiN films. This promotion of adhesion mainly resulted from ion beam mixing at the initial stage of film growth. The strong adhesion between RIBAD films and substrates obtained at ambient temperature is very beneficial to industrial application.

3.4.3. Wear behaviour

In order to investigate the wear behaviour of RIBAD TiN films, three TiN films with different thicknesses of 400, 1000 and 2000 nm, respectively, were tested on the pin-on-disc machine. Fig. 7a–d shows the wear traces on an uncoated SKD-11 substrate and the coated specimens; also shown in the figure are morphologies of spots of the corresponding counter parts. Without TiN coating, a wide, uneven and roughly peeled trace appears. Many crushed pieces stick on the ball. All these indicate that heavy wear occurred between the substrate and the counterpart. However, for specimens coated with TiN films, the wear traces became more and more smooth with increasing thickness of the films. The dimension of the traces and the spots also get smaller and smaller with increasing film thickness. Fig. 8 demonstrates the weight loss of the four samples after tribotesting. It can be seen easily that the weight loss of 2000 nm TiN film coated specimen is only one fourteenth of the uncoated substrate.

Fig. 9 shows the cross-sections of the wear traces after the SRV tribotest. It can be seen easily in Fig. 9a that the wear trace on the uncoated 9Cr18 steel substrate exhibits an arc, the depth is up to $8 \mu\text{m}$. However, the wear trace on the Xe^+ -RIBAD TiN film

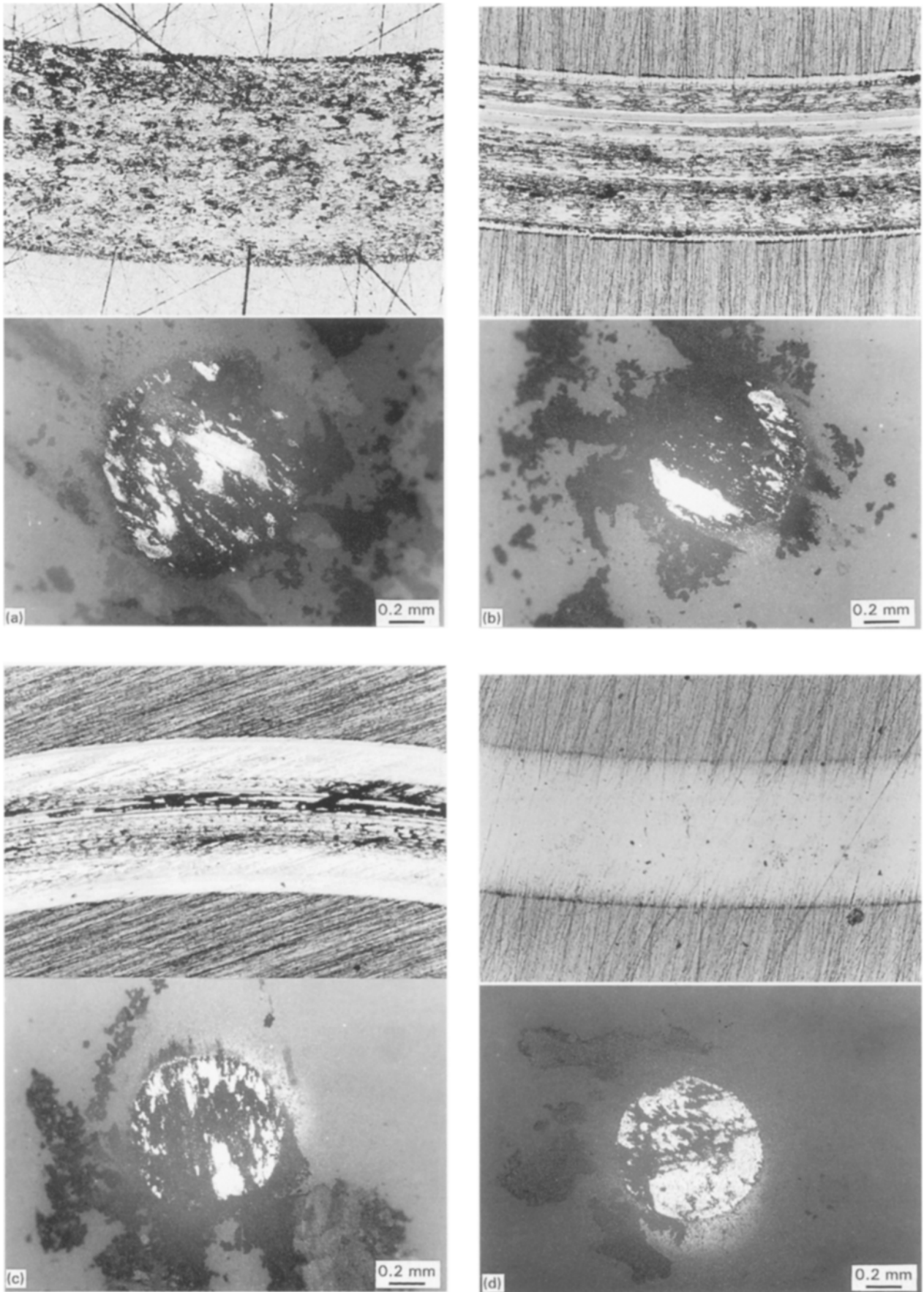


Figure 7 Wear traces on (a) substrate (SKD-11) and TiN films with thickness of (b) 400 nm, (c) 1000 nm, (d) 2000 nm, and spots of the corresponding counter parts.

is shallow, only 0.2 μm deep, as shown in Fig. 9b. So, it could be concluded that the wear resistance can be greatly improved by RIBAD TiN coatings.

3.5. Industrial application

Two kinds of scoring dies, which were used in a mint for producing silver alloy working pieces (type A) and

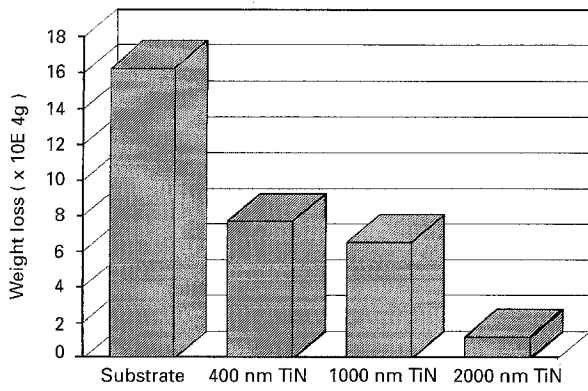


Figure 8 Weight loss of specimens corresponding to those in Fig. 7.

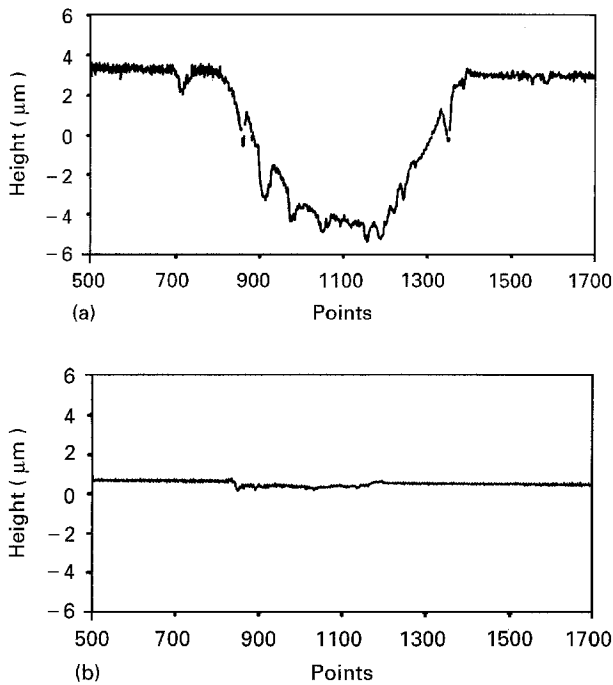


Figure 9 Cross-section of wear trace on (a) substrate (9Cr18) and (b) TiN film after SRV tribotesting.

in a die research centre for producing copper alloy working pieces (type B), respectively, were applied to industrial testing. Fig. 10 shows the surface morphology of a die of type A. These two kinds of scoring dies are very precise and cannot deal with high temperature procedure. Thus IBAD is a suitable technique to modify the dies, because it is a low temperature and highly controllable process.

Some scoring dies of type A were coated with 2000 nm thick TiN films by Xe⁺-RIBAD and others were plated with Cr. Then they were tested in practice on a 3.6×10^5 kgf punching machine without any lubricant applied to the surface of the dies. After having punched 300 silver alloy work pieces, highly concentrated small stick-like scratches, which could even be observed by eye, appeared on the surface of the dies plated with Cr (Fig. 11a). However, on the surface of RIBAD TiN coated dies, no apparent log-like scratch could be observed when 300 working pieces had been produced, and only slight scratches appeared as the yield was increased to 900 working pieces (Fig. 11b). The result proves that the service life of the dies coated



Figure 10 Surface morphology of a scoring die, type A.

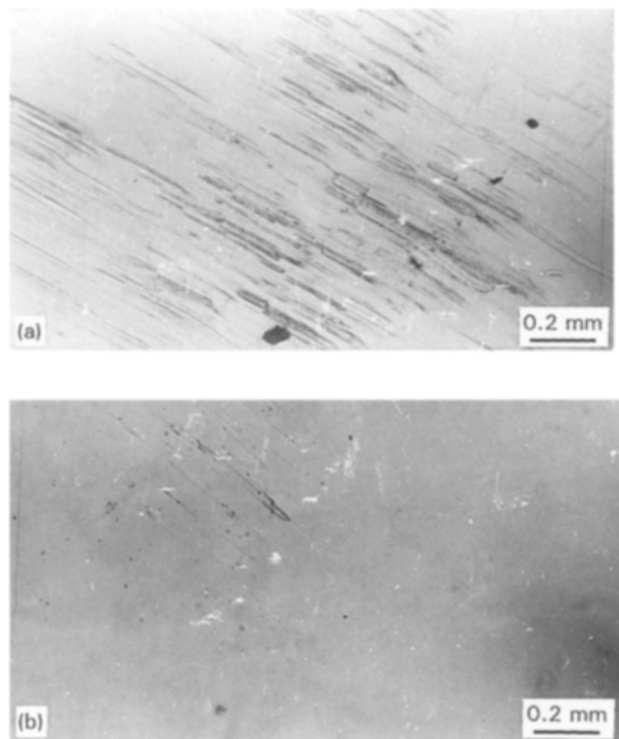


Figure 11 Micrographs of surfaces of dies (a) plated with Cr and (b) coated with TiN film after tests in practice.

with RIBAD TiN films can be increased more than three times.

As for dies of type B, the serious problem is that the dies normally tend to pick up copper from the working pieces, therefore requiring repolishing several times during their service lives. The RIBAD TiN coatings can greatly reduce the copper pick up, resulting in an increase of service life about five times.

4. Conclusions

Xenon ion beam assisted deposition of TiN film results in an increase in hardness compared to nitrogen ion beam assisted deposition, and very little content of xenon in the film. The deposited film is composed of homogeneous nanograins and presents slightly (200)

preferred orientation. A relative thick transition layer exists between the film and substrate. Even though formed at ambient temperature, the adhesion between the film and substrate is stronger than that between high temperature PVD film and substrate. The RIB-AD TiN film also exhibits excellent wear resistance. When applied to the scoring die industry, the TiN film can efficiently suppress surface damage of the dies, resulting in the extension of service life approximately five times.

References

1. F. A. SMIDT, *Int. J. Mater. Rev.* **35** (1990) 61.
2. G. K. HUBLER, *Critical Rev. Surf. Chem.* **2** (1993) 169.
3. P. J. MARTIN and R. P. NETHERFIELD, *Thin Solid Film* **239** (1994) 181.
4. R. N. BOLSTER, I. L. SINGER, R. A. KANT, B. D. SARTWELL and C.R. GOSSETT, *Surface Coating Technol.* **36** (1988) 781.
5. H. ITO, Y. YOSHIMA, S. YAMAJI, Y. MAEYAMA, T. INA and Y. MINOWA, *Nuclear Instrum. Meth. Phys. Res.* **B19/20** (1987) 644.
6. R. A. KANT, B. D. SARTWELL, I. L. SINGER and R. G. VARDIMAN, *ibid.* **B7/8** (1987) 915.
7. XI WANG, XIANGHUAI LIU, YOUSHAN CHEN, GENQING YANG, ZUYAO ZHOU, ZHIHONG ZHENG, WEI HUANG and SHICHANG ZOU, *Thin Solid Films* **202** (1991) 315.
8. XI WANG, GENQING YANG, XIANGHUAI LIU, ZHIHONG ZHENG, WEI HUANG, ZUYAO ZHOU and SHICHANG ZOU, *SPIE* **1519** (1991) 740.
9. XI WANG and P. MARTIN, *J. Mater. Sci. Lett.* **13** (1994) 1317.
10. XI WANG, GENQING YANG, XIANGHUAI LIU, ZHIHONG ZHENG, WEI HUANG and SHICHANG ZOU, *Mater. Sci. Eng* **A156** (1992) 91.
11. T. J. BELL, A. BENDELI, J. S. FIELD, M. V. SWAIN and E. G. THWAITE, *Metrologia* **28** (1991/92) 463.

*Received 22 December 1994
and accepted 2 May 1995*